Korea-Australia Rheology Journal
Vol. 13, No. 4, December 2001 pp. 197-203

Electrorheology and universal yield stress function of semiconducting polymer suspensions

Hyoung J. Choi*, Min S. Cho and Ji W. Kim
Department of Polymer Science and Engineering, Inha University, Incheon 402-751, Seoul Korea
(Received November 15, 2001)

Abstract

We reported on the eletrorheological (ER) properties of several semiconducting polymers including poly (p-phenylene) (PPP), poly (acene quinone) radicals (PAQRs), microencapsulated polyaniline (MPANI) and polyaniline (PANI) those we synthesized. The yield stress dependence on electric field strength for the ER fluids using these semiconducting polymers was mainly examined. The yield stress, which is an important design parameter for ER fluids, was observed to satisfy a universal scaling function, allowing that yield stress data for all the ER fluids examined in this study collapse onto a single curve for a broad range of electric field strengths. The proposed scaling function incorporates both the polarization and conductivity models.

1. Introduction

Electrorheological (ER) fluids are a class of materials whose rheological characteristics are controllable through the application of an electric field (Tao and Jiang, 1994). ER fluids are usually made of particle suspensions with a large dielectric constant mismatch between the particles and the fluid. Upon applications of an electric field, the suspended dielectric particles in an ER fluid align themselves into chains and columns parallel to the field, thereby inducing yield phenomenon, viscoelasticity, and a drastic increase in viscosity. (Ha and Yang, 1999) Because of their controllable viscosity and fast response, ER fluids are regarded as a smart material for active devices, which can transform electric energy to mechanical energy (See, 1999).

A wide variety of particulate materials have been employed in ER suspensions, including starch, flour, silica, alumina, titania, zeolite, and semiconducting polymers. Among these, the conventional hydrous ER particles such as starch, silica and alumina are known as wet-base systems because they require a small amount of water or some other polar molecule as an additive or promoter. The wet-base system has severe limitations in its engineering application, including thermal instability, water evaporation, corrosion of device and so on. Recently developed dry-base systems also exhibit the strong ER characteristics. Especially, the ER fluid based on semiconducting polymers is one of the novel, intrinsic ER systems. These include poly (acene quinone) radicals (Block *et al.*, 1990; Choi *et al.*, 1997a), polyaniline (Gow and Zukoski, 1989; Lee *et al.*, 1998; Choi *et al.*, 1999), phosphate cellulose (Kim *et al.*, 2001), copolypyrrole (Goodwin *et al.*, 1997), poly (p-phenylene) (Sim *et al.*, 2001), polyurethane (Bloodworth, 1994), N-substituted copolyaniline (Cho *et al.*, 1998), and polymer-clay nanocomposites with styrene-acrylonitrile copolymer (Kim *et al.*, 2000) or polyaniline (Kim *et al.*, 1999; Park *et al.*, 2001). These suspensions of semiconducting polymers show ER properties without any other additives, and polarization is induced with the movement of electrons in the molecules of particles under applied electric fields.

The main characteristics of ER fluids are a high yield stress and enhanced viscosity under an applied electric field, a response time on the order of milliseconds, and full reversibility, *i.e.* the fluid recovers its original properties when the electric field is removed. The yield stress is one of the critical design parameters in an ER device and has attracted considerable attention both experimentally (Duan *et al.*, 2000; Choi *et al.*, 1997; Wen *et al.*, 1997; See, 2000; Wu and Conrad, 1999; Chu *et al.*, 2000) and theoretically (Gonon *et al.*, 1999; Conrad *et al.*, 1999; Gully and Tao, 1997; Davis, 1997).

Furthermore, ER fluids with a yield stress under an externally applied electric field exhibit Bingham fluid behavior. Bingham fluid equation has been used as the suitable rheological model for the steady shear behavior of many ER fluids as described below:

$$\begin{aligned} \tau &= \tau_y + \eta\dot{\gamma} \qquad \tau \geq \tau_y \\ \dot{\gamma} &= 0 \qquad\qquad \tau < \tau_y \end{aligned} \tag{1}$$

Here, τ_y is the yield stress, which is a function of an electric field, τ is the shear stress, $\dot{\gamma}$ is the shear rate, and η shear

*Corresponding author: hjchoi@inha.ac.kr
© 2001 by The Korean Society of Rheology

viscosity. The $\dot{\gamma}=0$ in Eq. (1) can be noted that the extrapolation of $\dot{\gamma}$ to zero gives the dynmic yield stress τ_y^d under a controlled shear rate test.

Due to their significance, several models have been introduced to describe the ER phenomena via flow curve with a yield stress (Parthasarathy and Klingenberg, 1996; Gonon *et al.*, 1999; Conrad *et al.*, 1999). The original "polarization model", attributed the attractive force between particles to Maxwell-Wagners interfacial polarization and employed the point-dipole approximation (Parthasarathy and Klingenberg, 1996). Within this framework, the yield stress (τ_y) is represented as

$$\tau_y \propto \phi K_f E_0^2 f(\beta) \tag{2}$$

where ϕ is the volume fraction of the particles and $\beta = (K_p - K_f)/(K_p + 2K_f)$ is the dimensionless dielectric mismatch parameter. Here, K_p and K_f are the dielectric permittivities of the particle and the fluid, respectively. This polarization model shows excellent agreement (Parthasarathy and Klingenberg, 1996; Duan *et al.*, 2000) with data for small ϕ and E_0. However, yield stress data significantly deviate from Eq. (2) at high electric field strengths (Davis, 1997) and are better represented (Lee *et al.*, 1998; Wu and Conrad, 1999) by the power law; $\tau_y \propto E_0^m$ (m<2).

On the other hand, as the gap between the conducting particles in the fluid decreases, the electric response of the fluid becomes nonlinear through electrical breakdown or partial discharge under high electric field strengths. This nonlinear conductivity effect has been incorporated with the bulk conducting particle model (Davis, 1997) and an alternative yield stress model, showing that power law index "*m*" approaches 3/2 for high electric field strengths was thereby introduced.

Based on the nonlinear conductivity model for ER fluids (Davis, 1997), good agreement exists between predicted and measured ER behavior for various ER systems (Tang *et al.*, 1995a; Tang *et al.*, 1995b; Wu and Conrad, 1996; Wu and Conrad, 1997). Davis (1997) showed that over a range of unscaled E_0 greater than critical electric field (E_c), the slope of E_0 *vs.* τ_y (on log paper) is 3/2, while the slope approaches 2 for small E_0. Based on these observation, Choi *et al.*(2001) recently introduced the following simple hybrid equation to represent the yield stress data for a broad electric field strength range.

$$\tau_y(E_0) = \alpha E_0^2 \left(\frac{\tanh \sqrt{E_0/E_c}}{\sqrt{E_0/E_c}} \right) \tag{3}$$

where α depends on the dielectric constant of the fluid, the particle volume fraction, and β. E_c represents the critical electric field originated from nonlinear conductivity model, and is descriptive for crossover behavior and defines the two regimes in the E_0 *vs.* τ_y plot.

Equation (3) was found to give the following two limiting behaviors at low and high electric field strengths, respectively:

$$\tau_y = \alpha E_0^2 \quad \propto E_0^2 \qquad E_0 \ll E_c \tag{4a}$$

$$\tau_y = \alpha \sqrt{E_c} E_0^{3/2} \quad \propto E_0^{3/2} \qquad E_0 \gg E_c \tag{4b}$$

These equations show that τ_y is proportional to E_0^2 for low E_0, and τ_y changes abruptly to $E_0^{3/2}$ for high E_0.

In this study, using a generalized scaling function for the normalized yield stress via scaling of the applied electric field strengths, we extended its universality to various semiconducting polymer based ER suspensions.

2. Experimentals

2.1. Poly(p-phenylene)

The semiconducting PPP is known to be an insoluble, intractable, linear, rigid and infusible dark brown material with a low electric conductivity. In this study, the PPP particles were synthesized by adopting the procedure of Kovacic and Oziomek (1962). Under a nitrogen atmosphere and in the presence of aluminium chloride, water, and cupric chloride, which forms a Lewis acid, benzene was converted to PPP. The detailed synthesis process of PPP and its ER fluid preparation procedures were described in Sim *et al.* (2001). It has been also discovered that in most cases the synthesized PPP particles do not contain more than ten repeat units (Kovacic and Jones, 1987) because of the occurrence of side reactions, which destroy the functional groups and suppress the chain growth, and the occurrence of precipitating product from the solution (Schlüter and Wegner, 1993).

2.2. Poly (acene quinone) radicals

The PAQRs were synthesized following the method of Phol and Engelhardt (1962). Various kinds of acene monomers, such as anthrancene, naphthalene and pyrene, were used to synthesize a series of PAQRs (Choi *et al.* 1997a). Zinc chloride was used as catalyst for Friedel-Craft acylation between acenes and phthalic anhydride. To obtain uniform properties of the polymer, an inert gas atmosphere was used during the reaction, with degassing and maintenance of a vacuum state. The reaction temperature was 25°C and the reaction time was 24 hr. Prior to use, the polymer was ballmilled with a dilute HCL aqueous solution in order to remove the catalyst and to control the particle size. After milling, the mixture was sieved with a 38 μm sieve to control the particle size of the synthesized polymer particle, and then extracted into a Soxhlet apparatus, sequently with water, ethanol and benzene, to purify the products. Finally, the polymer was dried in a vacuum oven at room temperature.

2.3. Microencapsulated polyaniline

Despite its importance in the ER materials, PANI particles with low pH cannot be directly used in the ER sys-

tems, since their emerald base form has a conductivity that is too high. Therefore, the pH of the polyaniline has been controlled to yield a lower conductivity. To improve the particle preparation method for polyaniline, which generates ER fluids with its semiconducting characteristics, we synthesized microencapsulated polyaniline particles with melamine-formadehyde (MF) resins. Synthesized PANI particles were used as the core material for the encapsulation, and prepolymer MF as the shell materials. A mixture of 25 g of a 20% citric acid or poly (styrene sulfornic acid) and 100 g of distilled water was prepared. The pH of this solution was controlled to 4 with 1 M NaOH. Dried polyaniline particles were then put into this solution. After stirring this mixed solution for 2 hr at 40~45°C in a water bath, the solution of prepolymer melamine and 37% formaldehyde was added while stirring. As the temperature rose to about 65°C, MF resins were cured, and encapsulation of the polyaniline particles proceeded. After completion of the encapsulation reaction, the particles were filtered and washed with distilled water several times to remove the unreacted residuals. Finally, the products were dried in a vacuum oven at room temperature. Other encapsulated polyaniline samples were also prepared by varying the content of MF with a fixed molar ratio of melamine to formaldehyde. MPANI composites are denoted as MPANIn with n = 1, 2, 3. Here 1, 2, and 3 are related with thickness of MF resin. The ratios by weight of polyaniline to MF resin are 10/114 (MPANI1), 10/152 (MPANI2), and 10/190 (MPANI3), respectively

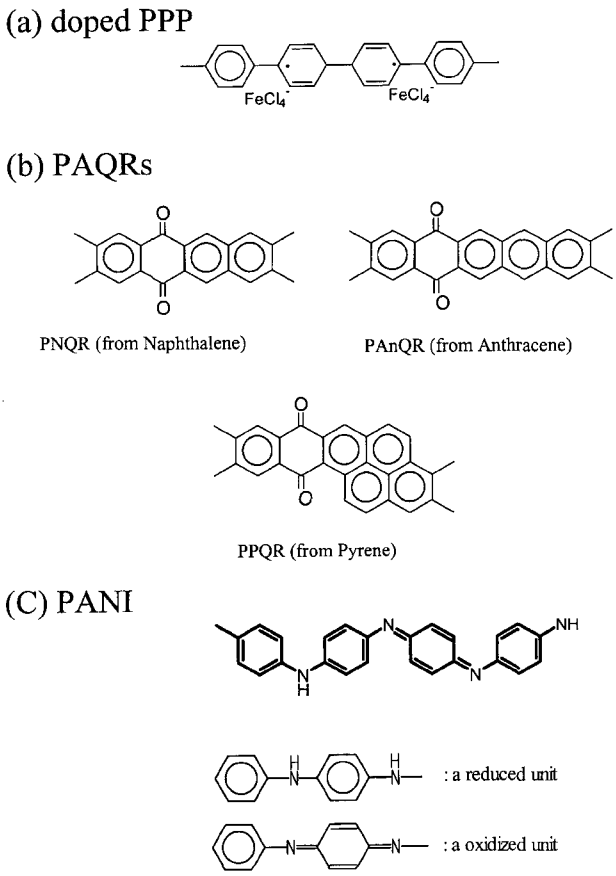

Fig. 1. Chemical structure of semiconducting polymers; (a) PPP, (b) PAQRs (c) PANI.

2.4. Characterization

General characterizations for the polymer particle were conducted by using Fourier transform-infrared spectroscopy (FT-IR) spectrum analysis for the characteristics of the chemical structure. Thermogravimetric analysis (TGA) showed that the thermal stability of the organic polymers was sustained. Scanning electron microscope (SEM) analysis was also used for observing the shape and size of the particles.

The kinematic viscosity and the density of the silicone oil were 30 cSt and 0.96 g/cm^3, respectively. Particle sizes and their distributions were measured by the particle size analyzer (Malvern MS 20, Malvern, UK) and particle shape was analyzed by scanning electron microscope (SEM S-2400, Hitachi, Hitachnaka, Japan). Density of the PPP particle was found to be 1.21 g/cm^3 by a pycnometer. The picoammeter (Keithley 487, Cleveland, USA) with custom-made cell (2 probes) was used to measure the conductivity of each sample pellets.

Fig. 1 shows chemical structures of various semiconducting polymers studied in this work. Generally, they have a phenyl ring structures, which give a route to conduct electron or have different polarities in the main polymer chain.

2.5. Rheological measurement

Rheological experiments were carried out using a rotational rheometer (Physica MC120, Stuttgart, Germany) with a Couette geometry (Z3-DIN and Z4-DIN), a high voltage generator (HVG 5000, Stuttgart, Germany), and an oil bath for temperature control. The gaps of Z3-DIN and Z4-DIN were 1.06 mm and 0.59 mm, and their maximum measurable stresses were 1.141 and 6.501 kPa, respectively. The HVG 5000 could supply DC voltage up to 5 kV within ± 10 μ. A of electric current. The suspensions were placed in the gap between the stationary outer measuring cup and the rotating bob. An electric field was applied for 3 minutes to obtain an equilibrium chainlike or columnar structure before applying shear. To obtain reproducible data, ER fluids were redispersed before each experiment, and measurements were carried out at least three times. The shear rate was varied from 10^{-2} to 10^2 s^{-1}, and yield stresses for the prepared ER fluids were mainly obtained under flow in a controlled shear rate (CSR) experiment. The stress of the transition point at which viscosity abruptly decreased was interpreted as the yield stress. Flow curves for each ER fluid were determined in the CSR

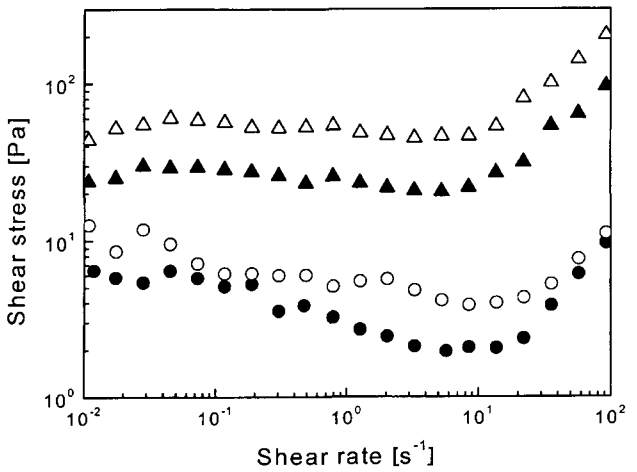

Fig. 2. Shear stress *vs.* shear rate for PPP(0.0) (●,▲) and PPP(5.0) (○,△) under different electric field strengths. (Circles are for 2 kV/mm and triangles for 3 kV/mm).

mode, and static yield stresses were obtained in controlled shear stress (CSS) mode.

3. Results and Discussion

Fig. 2 shows flow curves of shear stress *vs.* shear rate from the CSR experiment for 10 wt% suspensions of undoped PPP (0.0) and PPP (5.0) with different electric field strengths. In the absence of an electric field, ER fluids behave like an ordinary dilute suspension by showing a slight departure from Newtonian fluid behavior. When an electric field is applied to the suspension, the shear stress increases with increasing electric field strength, and τ_y becomes greater than zero (like in a Bingham fluid). In general, the structure in a concentrated suspension can be sufficiently rigid to permit the material to withstand a certain level of deforming stress without flowing. The maximum stress that can be sustained without flow is the yield stress. Doped suspensions, like the undoped ones, show similar behavior, such that the shear stress increases as electric field strength increases. It could be clearly seen that the shear stress of the doped suspension is larger than that of the undoped one. Note that the rheological measurements permit investigation of only a limited frequency range and electric field strength due to deformation, power supply capacity, and conductivity breakdown.

A correlation between the yield stress and electric field strength is represented in Fig. 3(a). τ_y is enhanced with the doping degree. On a log plot, the data show a linear relationship to the electric field strength (slope of 1.5). The PPP data are collapsed onto a single curve using Eq. (4), which is shown in Fig. 3(b). E_c is 1.5 kV/mm for PPP (0.0), 1.2 for PPP (2.5), 1.0 for PPP (5.0), and 0.9 for PPP (7.5).

On the other hand, Fig. 4(a) shows the yield stress for four different PPP volume fractions. The samples were

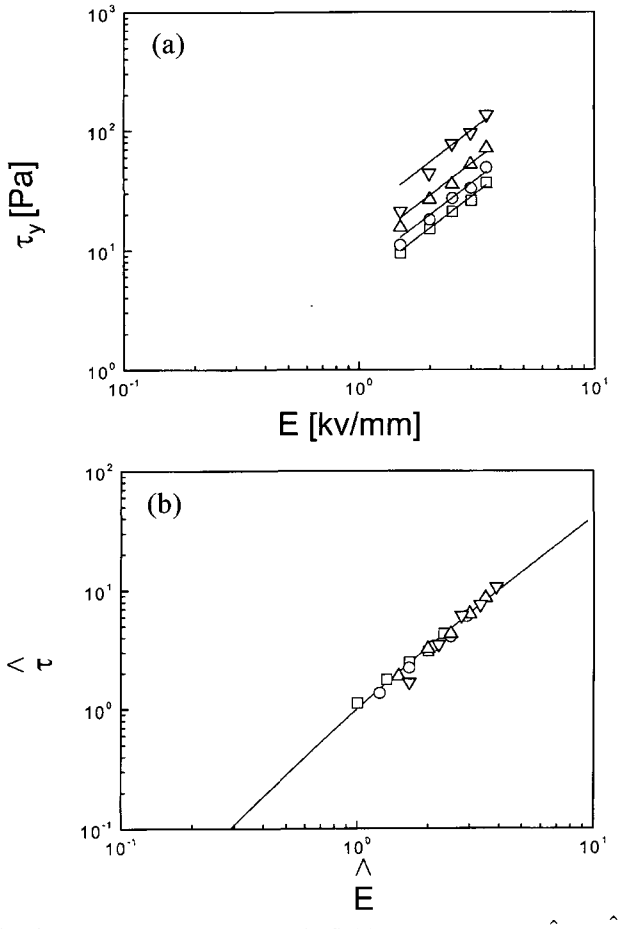

Fig. 3. (a) Yield stress *vs.* electric field strength and (b) $\hat{\tau}$ *vs.* $\hat{E}$ for □PPP (0.0), ○PPP (2.5), △PPP (5.0), and ▽PPP (7.5).

indexed to be PPP-1, PPP-2, PPP-3, and PPP-4 for 2.40, 4.01, 5.64, and 8.10 volume % of the PPP in silicone oil, respectively The static yield stress from a CSS test was performed for the PPP suspensions with six different electric field strengths (1.0, 1.5, 2.0, 2.5, 3.0, 3.5 kV/mm). As the volume fraction of doped PPP increases, the yield stress increases exponentially. The correlation between yield stress and electric field strength is represented. The yield stress is also enhanced by increasing the volume fraction. Generally, the correlation of the yield stress and electric field was presented as follows.

$$\tau_y \propto E^m \tag{5}$$

The "m" values for the PPP series were 2.0, 2.0, 1.96, and 1.73 respectively. The dependency of the yield stress on the electric field strength differs from the E^2 dependency suggested by the polarization model. The applied electric field induces electrostatic polarization interactions among the particles and also between the particles and the electrodes. However, the conduction model does not describe the flow effect accurately; that is, ER response is

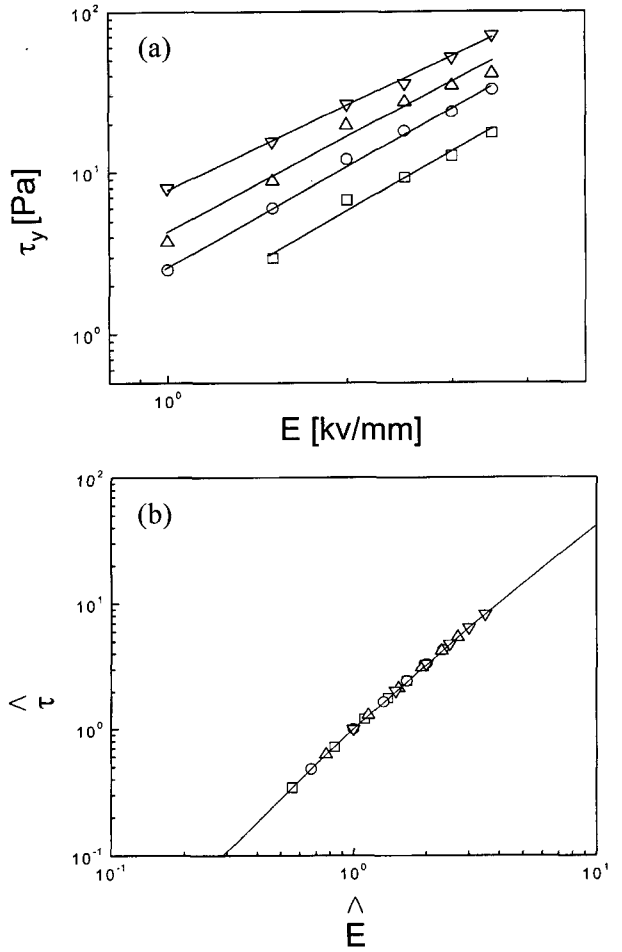

Fig. 4. (a) Yield stress vs. electric field strength for four different volume PPP suspensions with 5 wt% doping of $FeCl_3$ at 25°C (b) The universal curve for $\hat{\tau}$ vs. $\hat{E}$ for four different volume PPP suspensions (□PPP-1, ○PPP-2, △ PPP-3, ▽PPP-4).

influenced by the conductivity mismatch and the interaction between particle and medium. Various ER fluids show different exponents in Eq. (5). A correlation between yield stress and electric field strength is represented in Fig. 4(b).

Fig. 5 shows our data for an ER fluid consisting of microencapsulated polyaniline (MPANI) with a melamine-formaldehyde (MF) resin dispersed in silicon oil, which are in excellent agreement with Eq. (3). Ec for different MPANI composites are 1.09 (MPANI1), 1.07 (MPANI2), and 1.05 (MPANI3) kV/mm, respectively. Corresponding conductivities are 1.11×10^{-11}, 5.09×10^{-12}, and 2.39×10^{-12} S/cm, respectively. Therefore, E_c appears to be proportional to the particle conductivity. In our preliminary investigation with various ER fluid data, we also found that E_c is influenced by the conductivity mismatch between the particle and medium liquid and is weakly dependent on the volume fraction.

To collapse the data into a single curve, we normalized

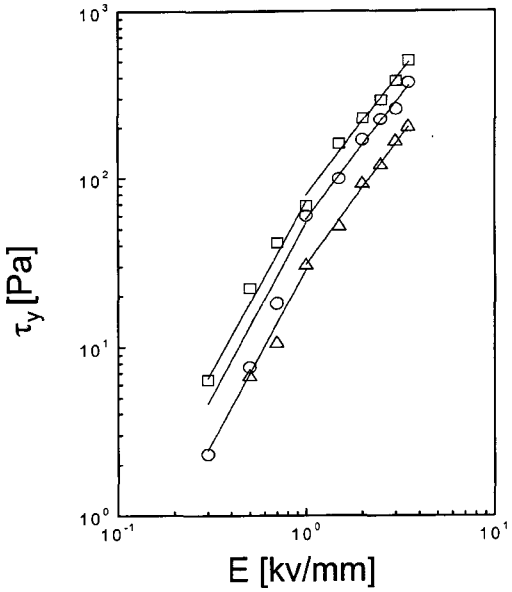

Fig. 5. τ_y *vs.* E_0 for 20 wt% suspensions of MPANI particles encapsulated with MF resin (□MPANI1, ○MPANI2, △ MPANI3).

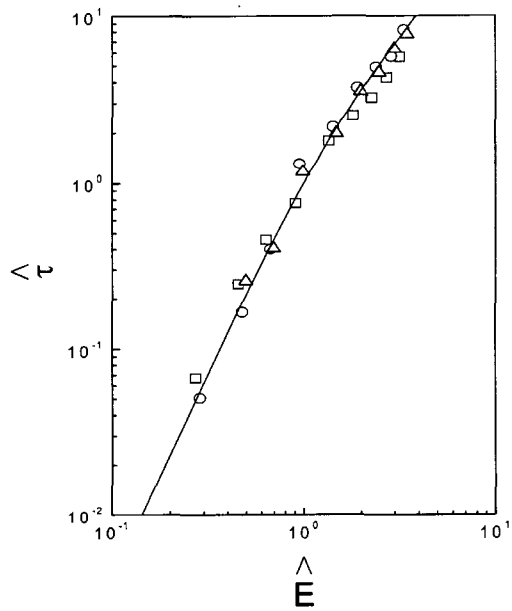

Fig. 6. $\hat{\tau}$ *vs.* $\hat{E}$ for 20 wt% suspensions of MPANI particles encapsulated with MF resin in silicone oil. The line is obtained from Eq. (6). (□MPANI1, ○MPANI2, △MPANI3).

Eq. (3) with E_c and $\tau_y(E_c) = \alpha E_c^2 \tanh(l) = 0.762\alpha E_c^2$:

$$\hat{\tau} = 1.313\hat{E}^{3/2}\tanh\sqrt{\hat{E}} \tag{6}$$

where $\hat{E} \equiv E_0/E_c$ and $\hat{\tau} \equiv \tau_y(E_0)/\tau_y(E_c)$.

The data shown in Fig. 5 collapsed onto a single curve by using Eq. (6). Fig. 6 represents these collapsed data.

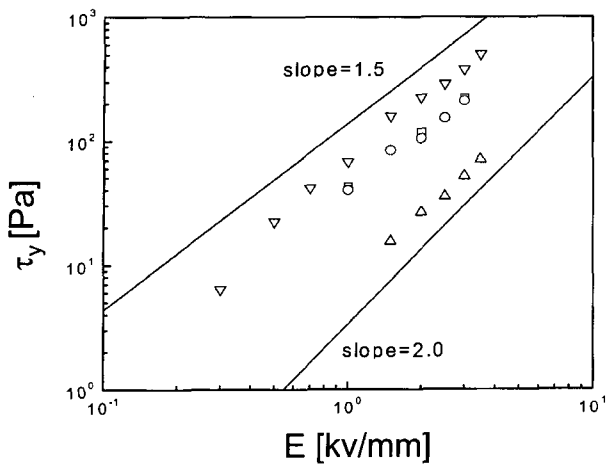

Fig. 7. τ_y *vs.* E_0 for ER fluids using various semiconducting polymers (□PANI, ○PNQR, △PPP, ▽MPANI).

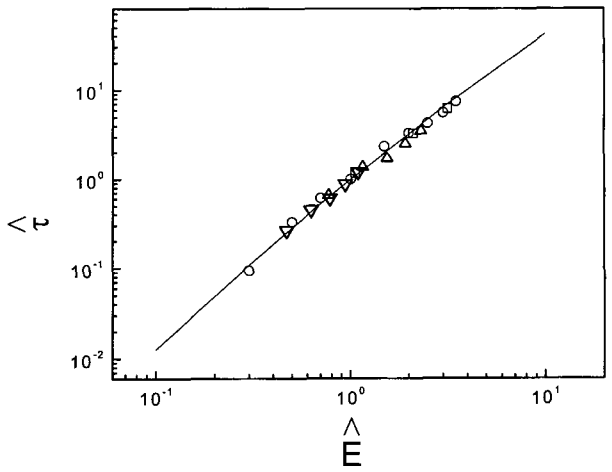

Fig. 8. $\hat{\tau}$ *vs.* $\hat{E}$ for ER fluids using various semiconducting polymers (□PANI, ○PNQR, △PPP, ▽MPANI).

Table 1. Summary of information on ER fluids adopted in this work

Code	Particle	Conc.[1]	σ[2] [S/cm]	E_0 range [kV/mm]	m[3]	E_c[4] [kV/mm]
PANI	Polyaniline	10 vol%	10^{-11}	1.0 ~ 3.0	1.5	0.95
MPANI	Microencapsulated polyaniline[5]	about 15 vol%	-	0.3 ~ 1.0 0 ~ 3.5	1.5 2.0	1.0
PNQR	poly (naphthalene quinone) radical	15 vol%	3.3×10^{-7}	1.0 ~ 3.0	1.5	1.3
PPP	poly(p-phenylene)	about 5 vol%		1.5 ~ 3.5	2.0	3.2

[1]particles in silicone oil.
[2]particle conductivity.
[3]exponent in equation of $\tau_y \sim E_0^m$.
[4]obtained from Eq. (4).
[5]core : polyaniline ($\sigma > 10^{-7}$ S/cm), shell: melamine-formaldehyde resin.

On the other hand, Fig. 7 shows yield stress (τ_y) data for all ER fluids using several semiconducting polymers as a function of electric fields (E_0). Poly (naphthalene quinone) radical (PNQR) (Choi *et al.*, 1997a) based ER fluids shows a relationship between τ_y and E_0 as $\tau_y \sim E_0^{1.5}$. Poly (p-phenylene) (PPP) (Sim *et al.*, 2001) based ER fluids have $\tau_y \sim E_0^{2.0}$. In the case of MPANI ER fluid (Choi *et al.*, 2000), the exponent was 2.0 below 1 kV/mm and 1.5 above 1 kV/mm. Various properties of these ER fluids summarized in Table 1.

Finally, the data for ER fluids using various semiconducting polymers are found to collapse onto a single curve by using Eq. (6) (Fig. 8). Thereby, we believe that Eq. (6) is a very useful expression in constructing the master yield stress curve for ER fluids. The beauty of these correlations is the fact that most of the ER experimental data can be collapsed with one parameters (E_c).

Furthermore, for the different particle volume ratios or doping degree, scaling equation fitted well in case of PPP based ER fluid. From these results, it was found that the proposed universal scaling equation is well fitted to most ER systems.

Acknowledgements

This work was supported by research grants from the Korea Science and Engineering Foundation (KOSEF) through the Applied Rheology Center (ARC), an official KOSEF-created engineering research center (ERC) at Korea University, Seoul Korea.

References

Block, H., J. P. Kelly, A. Qin, and T. Waston, 1990, *Langmuir* **6**, 6.

Bloodworth, R., 1994, Electrorheological Fluids, Mechanisms, Properties, Technology and Applications, World Scientific, Singapore, p.67.

Cho, M. S., H. J. Choi, and K. To, 1998, *Macromol. Rapid Commun.* **19**, 271.

Choi, H. J., M. S. Cho, and M. S. Jhon, 1997a, *Polym. Adv. Tech.* **8**, 697.

Choi, H. J., J. H. Lee, M. S. Cho, and M. S. Jhon, 1999a, *Polym.*

Eng. Sci. **39**, 493.
Choi, H. J., Y. H. Lee, C. A. Kim, and M. S. Jhon, 2000, *J. Mater. Sci. Lett.* **19**, 533.
Choi, H. J., J. W. Kim, and K. To, 1999b, *Polymer* **40**, 2163.
Choi, H. J. M. S. Cho, J. W. Kim, C. A. Kim and M. S. Jhon, 2001, *Appl. Phys. Lett.* **78**, 3806.
Chu, S. H, K. H. Ahn and S. J. Lee, 2000, *J. Rheol.* **44**, 105.
Conrad, H., C. W. Wu, and X. Tang, 1999, *Intl. J. Mod. Phys. B* **13**, 1729.
Davis, L. C., 1997, *J. Appl. Phys.* **81**, 1985.
Duan, X., H. Chen, Y. He, and W. Luo, 2000, *J. Phys. D: Appl. Phys.* **33**, 696.
Grem, G., G. Leditzky, B. Ullrich, and G. Leising, G. 1992, *Adv. Mater.* **4**, 36.
Grem, G., V. Martin, F. Meghdadi, C. Paar, J. Stampfl, J. Sturm, S. Tasch, G. Leising, 1995, *Synth. Met.* **71**, 2193.
Goldenberg, L. M. and P. C. Lacaze, 1993, *Synth. Met.* **58**, 271.
Gonon, P., J.-N. Foulc, P. Atten, and C. Boissy, 1999, *J. Appl. Phys.* **86**, 7160.
Goodwin, J. W., G. M. Markham, and B. Vinent, 1997, *J. Phys. Chem. B* **101**, 1961.
Gow, C. J. and C. F. Zukoski, 1989, *J. Colloid Inter. Sci.* **136**, 175.
Gulley, G. L. and R. Tao, 1997, *Phys. Rev. E* **56**, 4328.
Ha, J. W. and S. M. Yang, 1999, Korea-Australia Rheol. J. 11, 241.
Kim, J. W., S. G. Kim, H. J. Choi, and M. S. Jhon, 1999, *Macromol. Rapid Commun.* **20**, 450.
Kim, J. W., M. H. Noh, H. J. Choi, D. C. Lee, and M. S. Jhon, 2000, *Polymer* **41**, 1229.
Kim, J. W., H. J. Choi, S. H. Yoon, and M. S. Jhon, 2001a, *Int. J. Mod. Phys. B* **15**, 634.
Kim, S. G., J. W. Kim, W. H. Jang, H. J. Choi, and M. S. Jhon, 2001b, *Polymer* **42**, 5005.
Kovacic, P and J. Oziomek, 1962, *J. Am. Chem. Soc.* ***85***, 454.
Kovacic, P and M. B. Jones, 1987, *Chem. Rev.* ***87***, 357.
Lee, H. J., B. D. Chin, S. M. Yang and O. O. Park, 1998 *J. Colloid Inter. Sci.* **206**, 424.
Park, J. H., Y. T. Lim and O. O. Park, 2001, *Macromol. Rapid Commun.* **22**, 616.
Parthasarathy, M. and D. J. Klingenberg, 1996, *Mater. Sci. Eng* **R17**, 57.
Phol, H. A. and E. H. Engelhardt, 1962, *J. Phys. Chem.* **66**, 2085.
Plocharski, J., M. Rozanski, H. Wycislik, 1999, *Synth. Met.* **102**, 1354.
See H., 1999, *Korea-Australia Rheol. J.* **11**, 169.
See, H., 2000, *J. Phys. D: Appl. Phys.* **33**, 1623.
Sim, I. S., J. W. Kim, H. J. Choi, C. A. Kim, and M. S. Jhon, 2001, *Chem. Mater.* **13**, 1243.
Schlûter, A. D. and G. Wegner, 1993, *Acta. Polym.* ***44***, 59.
Tang, X., C. W. Wu, and H. Conrad, 1995a, *J. Rheol.* **39**, 1059.
Tang, X., C. W. Wu, and H. Conrad, 1995b, *J. Appl. Phys.* **78**, 4183.
Tao, R. and Q, Jiang, 1994, *Phys. Rev. Lett.* **73**, 205.
Wen, W., N. Wang, W. Y. Tam, and P. Sheng, 1997, *Appl. Phys. Lett.* **71**, 2529.
Wu, C. W. and H. Conrad, 1996, *J. Phys. D* **29**, 3147.
Wu, C. W. and H. Conrad, 1997, *Phys. Rev. E* **56**, 5789.
Wu, C. W. and H. Conrad, 1999, *Intl. J. Mod. Phys. B* **13**, 1713.